Pd L_3-Edge XANES Spectra of Supported Pd Particles Induced by the Adsorption and the Absorption of Hydrogen

Takeshi Kubota, Yoshinori Kitajima,† Kiyotaka Asakura,†† and Yasuhiro Iwasawa*

Department of Chemistry, Graduate School of Science, The University of Tokyo, 7-3-1, Hongo, Bunkyo-ku, Tokyo 113-0033

†Photon Factory, Institute of Materials Structure Science, High Energy Accelerator Research Organization, Oho 1-1, Tsukuba, Ibaraki 305-0801

††Research Center for Spectrochemistry, Graduate School of Science, The University of Tokyo, 7-3-1, Hongo, Bunkyo-ku, Tokyo 113-0033

(Received October 9, 1998)

We measured Pd L_3-edge X-ray absorption near-edge structure (XANES) spectra for small Pd particles dispersed on inorganic oxide supports (SiO_2 and Al_2O_3) and the spectra changes induced by the adsorption and the absorption of hydrogen. When the XANES spectra were measured under the atmosphere of H_2, a new peak appeared at about 8 eV above the inflection point of the absorption edge. The peak position was invariant but its intensity decreased with the decrease of Pd particle size. This peak is caused by hydrogen absorption in the Pd particles. Hydrogen at the subsurface region little affected the Pd L_3-edge XANES spectra. A new peak also appeared for the Pd sample accompanied with hydrogen adsorbed on the surface. The peak energy relative to the edge was independent of the Pd particle size and the peak intensity increased with the amount of adsorbed hydrogen. The XANES spectra can quantify the adsorbed and absorbed hydrogen atoms. We presented a model of Pd particles composed of surface, subsurface and bulk atoms.

X-Ray absorption near-edge structure (XANES) is explained by the electron transition from a core level to unoccupied valence levels or by multiple scattering between an X-ray absorbing atom and surrounding atoms.[1,2] Since XANES reflects the electronic and local geometrical structures of an X-ray absorbing atom, it has been used to determine symmetry, bond distance and electronic state around the absorbing atom.

The $L_{2,3}$-edge XANES spectra of transition metal elements with unoccupied d states show a strong peak just above the absorption edge; this is called the white line. As the white line is assigned to a transition from 2p core level to unoccupied nd states, $L_{2,3}$-edge XANES has been used to estimate the density of the unoccupied d-states of X-ray absorbing atoms;[3—5] the results are used to investigate the electronic structure of supported Pt small particles.[4,6]

Moreover, the large penetration power of X-rays enables us to carry out in-situ XANES measurements in the presence of a reaction gas.[4,7,8] Yoshitake et al. studied the change of electronic states in Pt particles by the adsorption of various kinds of gas systematically by means of the Pt $L_{2,3}$-edge XANES.[7] When hydrogen adsorbs on highly dispersed Pt particles on oxide surfaces, the Pt $L_{2,3}$-edge peaks are broadened to the higher energy side and a new peak appears at about 8 eV from the edge in difference spectra obtained by subtracting the spectra for clean samples from those for samples adsorbed with hydrogen.[8—13] The origin of such H-induced change of XANES has been discussed in terms of several mechanisms involving metal-support interaction,[9,11] Pt-hydrogen antibonding,[10,13,14] and change of multiple scattering effects induced by hydrogen adsorption.[15] In our previous papers on supported Pt particles, we reported that the photon energy of the peak in the Pt L_3-XANES difference spectra before and after H_2 adsorption was independent of the amount of adsorbed hydrogen, the size of Pt particles, and the kind of supports.[16—18] Moreover the peak intensity was proportional only to the amount of adsorbed hydrogen. Thus we have proposed that the intensity of the peak in the difference spectra can be used as a new way to analyze the amount of adsorbed hydrogen on supported Pt particles in vacuo and under the conditions relevant to catalytic reactions.[16—18]

It is of interest whether or not this method can be extended to adsorbed hydrogen on other noble metals. In this paper we will report the change of XANES spectra for small Pd particles on SiO_2 induced by hydrogen. In contrast to Pt, Pd absorbs hydrogen into the bulk to form Pd hydride and thereby acts as a medium for hydrogen storage. The Pd hydride systems have also been studied in relation to catalytic hydrogenation reactions.[19—26] Hydrided Pd catalysts may be resistant to coke formation.[26,27] Davoli et al. measured Pd L_3-edge XANES spectra of Pd films with absorbed hydrogen.[28] A change in the spectral feature induced by absorbed hydrogen was observed at 5.6 eV above the white line peak (about 8 eV above the absorption edge). Soldatov et al. compared the measured spectra with the spectra calculated by multiple scattering, and concluded that the spectral change induced by

hydrogen could be explained by a multiple scattering theory between an X-ray absorbing Pd atom and hydrogen atoms though hydrogen itself is a weak scatterer.[29] But there is little study about Pd L-edge XANES of supported Pd particles and their interaction with H_2. The purpose of this work is to investigate the change of XANES spectra for small Pd particles on inorganic oxides upon H_2 adsorption and absorption and to develop a new characterization method to determine the amount of adsorbed/absorbed hydrogen on/in Pd particles using XANES spectra.

Experimental

Sample Preparation. SiO_2 (Nippon Aerosil, Aerosil 300; surface area:300 $m^2\ g^{-1}$) and Al_2O_3 (Nippon Aerosil, Alon C; surface area:100 $m^2\ g^{-1}$) were used as supports. High dispersion Pd/SiO_2 samples were obtained by an ion-exchange method. In the ion-exchange method, the pH of aqueous suspensions of SiO_2 was regulated to be 9.1 by adding an aqueous solution of NH_3 in order to exchange protons of hydroxyl groups on SiO_2 by ammonium ions. Then the supports were impregnated with an aqueous solution of $[Pd(NH_3)_4]Cl_2$ (Soekawa Chemical Co.), followed by filtering and washing with water until the filtrate pH becomes 7.0. The obtained samples were dried at 393 K and calcined at 573 K in a flow of O_2. The Pd loading was 1.0 wt%. A high dispersion Pd/Al_2O_3 was obtained by using an impregnation of $[Pd(acac)_2]$ (Hacac = acetylaceton) acetone solution with Al_2O_3, which was then dried at 393 K and calcined at 573 K. An impregnation method using an aqueous solution of $Pd(NO_3)_2$ was employed to prepare low dispersion Pd/SiO_2 and Pd/Al_2O_3 samples, followed by calcination at 673 K in air.

The samples thus obtained were placed in a U-shaped Pyrex glass tube combined in a closed circulating system, and calcined with oxygen of 13.3 kPa at 573 K, followed by reduction with hydrogen of 13.3 kPa and evacuation at temperatures given in Table 1. The amounts of adsorbed hydrogen and CO relative to Pd atoms in the particles (H_{ad}/Pd and CO/Pd) were determined from irreversible uptakes of hydrogen and CO at 293 K, respectively. The method proposed by Boudart et al.[31] was adopted for the adsorption measurement of hydrogen on Pd particles. The hydrogen uptake was measured at P_{H2} = 13.3 kPa. The equilibrium pressure was determined when no change in the H_2 pressure was observed for more than 1 h. After the first hydrogen adsorption measurement, the system was evacuated for 1 h at room temperature. During the evacuation at room temperature, absorbed hydrogen was removed, while the adsorbed hydrogen remained on the surface. Then the second hydrogen uptake was measured and the irreversible hydrogen uptake was regarded as the difference of the two values. Chemisorbed CO was also measured similarly. The ratio of absorbed hydrogen to Pd in the particles was estimated by the second hydrogen uptake measurement at room temperature because the absorbed hydrogen was removed by the evacuation at room temperature.[30,31]

XANES Measurements and Analysis. Pd L_3-edge XANES spectra were measured in a fluorescence mode at BL-11B of the Photon Factory in Institute of Materials Structure Science, High Energy Accelerator Research Organization (KEK-IMSS-PF). The storage ring was operated at 2.5 GeV and the ring current was 300 mA. The synchrotron radiation was monochromatized by a Ge(111) double-crystal monochromator.[32] The higher harmonics were eliminated using a Ni-coated total reflection mirror. The estimated energy resolution near Pd L_3-edge was about 0.7 eV. The fluorescence detection (I_f) was carried out by using a gas-flow proportional counter[33] filled with Kr/C_2H_6 = 90/10 mixed gas. The 1900 V bias was applied to the electrode of the proportional counter. The incoming X-ray (I_0) was monitored by the photocurrent from a metal mesh placed before the samples. The sample was treated in a closed circulating system and transferred to a cell with two Kapton windows (25 μm) without contacting air, then stored in a N_2 filled reservoir till the measurement. Those cells were placed in a high vacuum chamber (5—8×10^{-6} Torr, 1 Torr = 133.322 Pa) which is installed with the fluorescence detector. The XANES spectra of the supported Pd particles were measured under three different conditions, i.e., under vacuum, in the presence of 13.3 kPa of hydrogen, and after subsequent evacuation at room temperature for 1 h, which are denoted as Pd/SiO_2(VAC), $Pd/SiO_2(H_2)$, and Pd/SiO_2(EVAC), respectively. The X-ray absorbance, μt was obtained from collected data I_f and I_0 by Eq. 1:

$$\mu t = I_f/I_0 \quad (1)$$

The pre-edge background subtraction was carried out by extrapolating the data in the pre-edge region (3096—3165 eV) to higher energy with a straight line and the data was normalized by the edge height. The inflection point of the absorption edge of Pd powder (3172.8 eV) was used for energy calibration.

We discriminated between the effects of adsorbed and absorbed hydrogen, using the behavior of absorbed hydrogen that is easily removed by room-temperature evacuation.

EXAFS Measurement. Pd K-edge EXAFS spectra of Pd/SiO_2 samples were measured at BL-10B in the Photon Factory in a transmission mode at room temperature. The synchrotron radiation was monochromatized by a Si(311) channel-cut monochromator at BL-10B. The estimated energy resolution near Pd K-edge was about 7 eV. The incident and transmitted X-ray intensities were detected by ion chambers filled with Ar gas for I_0 and with Kr gas for I. The voltages applied to electrodes were 500 V. The EXAFS data were analyzed using the Rigaku EXAFS (REX). The analysis involves

Table 1. Amounts of Adsorbed/Absorbed Hydrogen and Adsorbed CO per Pd Atom on Pd/SiO_2 and Pd/Al_2O_3

Support	Precursor	Loading	Reduction	H_{ad}/Pd	CO/Pd	H_{ab}/Pd
		wt%	temp/K			
SiO_2						
Aerosil 300	$[Pd(NH_3)_4]Cl_2$	1.0	573	0.74	0.44	0.33
Aerosil 300	$[Pd(NH_3)_4]Cl_2$	1.0	773	0.56	0.32	0.45
Aerosil 300	$Pd(NO_3)_2$	0.9	673	0.29	0.12	0.48
Aerosil 200	$Pd(NO_3)_2$	2.3	773	0.12	0.07	0.54
Al_2O_3						
Alon C	$[Pd(acac)_2]$	0.81	573	0.81		
Alon C	$Pd(NO_3)_2$	2.3	773	0.20		

preedge extrapolation, background removal by a spline smoothing method to extract EXAFS oscillation.[34] Then EXAFS data were Fourier transformed from k space(30—140 nm^{-1}) to r space. An inverse Fourier transformation was performed in the range of 0.17—0.30 nm to filter out the Pd–Pd first nearest neighbor contribution. The data were analyzed by a curve fitting procedure to obtain the coordination number N, bond distance r and Debye–Wallor factor σ, E_0 using Eqs. 2 and 3:

$$k^3\chi(k) = k^2NF(k)\exp(-2\sigma^2k^2)\sin(2kr + \phi(k))/r^2, \quad (2)$$

where k is the wave number of a photoelectron and is expressed by Eq. 3.

$$k = \sqrt{2m/\hbar^2(E - E_0)}, \quad (3)$$

where m is the mass of an electron, and E and E_0 are X-ray photon energy and threshold energy for photoemission, respectively. The backscattering amplitude $F(k)$ and phase shift $\phi(k)$ for Pd–Pd bond were extracted from the EXAFS data of Pd foil with r(Pd–Pd) = 0.276 nm and $N = 12$. σ and E_0 are tentatively set to 0.006 nm and 0 eV. The degree of fitting was estimated by the R factor (R_f) described below.

$$R_f = \sqrt{\sum(\chi_{obs}(k) - \chi_{cal}(k))^2} \Big/ \sqrt{\sum\chi_{obs}(k)^2} \quad (4)$$

Results

H_2 Adsorption and Absorption and CO Adsorption. H_{ad}/Pd (number of adsorbed hydrogen per Pd atom), CO/Pd (number of adsorbed CO per Pd atom) and H_{ab}/Pd (number of absorbed hydrogen per Pd atom) are given in Table 1. Although there is a correlation between the H_{ad}/Pd and CO/Pd, H_{ad}/Pd is always larger than CO/Pd, because the amounts of adsorbed CO and H_2 at saturation are different from each other and the CO adsorbed on Pd surface involves both linear and bridge types, as previously reported. H_{ad}/Pd has been used as a measure of metal dispersion or fraction of surface-exposed metal atoms, assuming a stoichiometry of $H_{ad}/Pd_s = 1$ (Pd_s:surface Pd atoms).[30,31,34] Since we found that Pd particles similarly prepared took a spherical shape on SiO_2 by TEM in a previous work and the averaged particle size derived from TEM agreed with that obtained from H_{ad}/Pd,[36] we estimated the size of Pd particles from the H_{ad}/Pd values assuming a spherical shape of the particles (Table 2). The amounts of absorbed hydrogen (H_{ab}/Pd) decreased with a decrease of particle size, as shown in Table 1. The relation between H_{ab}/Pd and H_{ad}/Pd in this work well corresponds to the literature data.[30]

Table 2. Particle Sizes Estimated from Adsorption of H_2(H_{ad}/Pd) and EXAFS Coordination Number

H_{ad}/Pd	d^*/nm	d^{**}/nm
0.74	1.6	1.0±0.8
0.56	2.2	1.2±1.4
0.29	4.0	1.6±2.0
0.12	9.5	N. D.

d^*: from H adsorption, d^{**}: from EXAFS, N.D.: The size could not be determined by EXAFS.

Results of EXAFS. The EXAFS oscillations and their Fourier transforms for Pd/SiO_2(VAC), Pd/SiO_2(H_2), and Pd/SiO_2(EVAC) are shown in Figs. 1 and 2, respectively. The curve fitting results are tabulated in Table 3. In Pd/SiO_2(VAC) with H/Pd = 0.74, 0.56, 0.29, and 0.12, the Pd–Pd distances (0.275±0.002 nm) were similar to that for Pd bulk (0.276 nm). The structural parameters such as coordination number, distance and Debye–Wallor factor for Pd/SiO_2(EVAC) are the same within the limits of error as those of the Pd/SiO_2(VAC).

We estimated the average size of Pd particles from the coordination number using a Greegor and Lytle method assuming the spherical shape.[37] In the present study, the coordination numbers of Pd/SiO_2(EVAC) were used for the estimation. The results are given in Table 2. The particle sizes derived from the EXAFS coordination numbers are a little smaller than those estimated from the adsorption of hydrogen (H_{ad}/Pd), but both values are compatible if the error bars are taken into account.

In Pd/SiO_2(H_2) samples, the Pd–Pd distances increased compared with those for Pd/SiO_2(VAC); this distance increased from 0.275 nm for Pd/SiO_2(VAC) up to 0.284 nm for Pd/SiO_2(H_2) with H_{ad}/Pd = 0.12. The increase of Pd–Pd distance in Pd/SiO_2(H_2) is due to the Pd lattice expansion induced by the hydrogen absorption. The Pd–Pd distance in bulk PdH_x ($x = 0.6$) is known to be 0.2855 nm, which is similar to the values for Pd–Pd in Pd/SiO_2(H_2) with H_{ad}/Pd = 0.12. The Pd–Pd distances in the Pd/SiO_2 samples with H/Pd = 0.75 and 0.56. Increased after hydrogen absorption, indicating that small Pd particles can absorb hydrogen. Interestingly, the increase in the Pd–Pd distance becomes smaller with the smaller Pd particle size. When the samples were evacuated at room temperature for 1 h (Pd/SiO_2(EVAC)), the Pd–Pd bond distances decreased to 0.275–0.277 nm shown in Table 3, indicating that the absorbed hydrogen in all the samples was removed by evacuation at room temperature.

XANES Spectra of Pd/SiO_2 under Interaction of Hydrogen. Figures 3, 4, 5, and 6 show Pd L_3-edge XANES spectra for the Pd/SiO_2 samples with the dispersions (H_{ad}/Pd) of 0.74, 0.56, 0.29, and 0.12, respectively. Each figure contains three sets of the XANES spectra for Pd/SiO_2(VAC), Pd/SiO_2(H_2), and Pd/SiO_2(EVAC). The white line peak for Pd/SiO_2(VAC) before exposing to H_2 increased with the decrease in particle size. The white line is caused by the transition from 2p to unoccupied 4d states of Pd. If the transition dipole moment is the same, the intensity of the white line peak indicates the amount of unoccupied d states of the Pd atoms.[4–6] The results in Figs. 3, 4, 5, and 6 indicate that the electron density of d-states for Pd particles decreases with the decrease of the particle size, which agrees with the literature.[38] After exposing Pd/SiO_2(VAC) to hydrogen, the white line peak decreased and the absorption coefficient around 3181 eV increased instead. Especially in low dispersion samples, a new definite peak appeared at about 3181 eV in the presence of gas phase H_2 (Figs. 5 and 6). The new peak decreased in height and is broadened with the increase

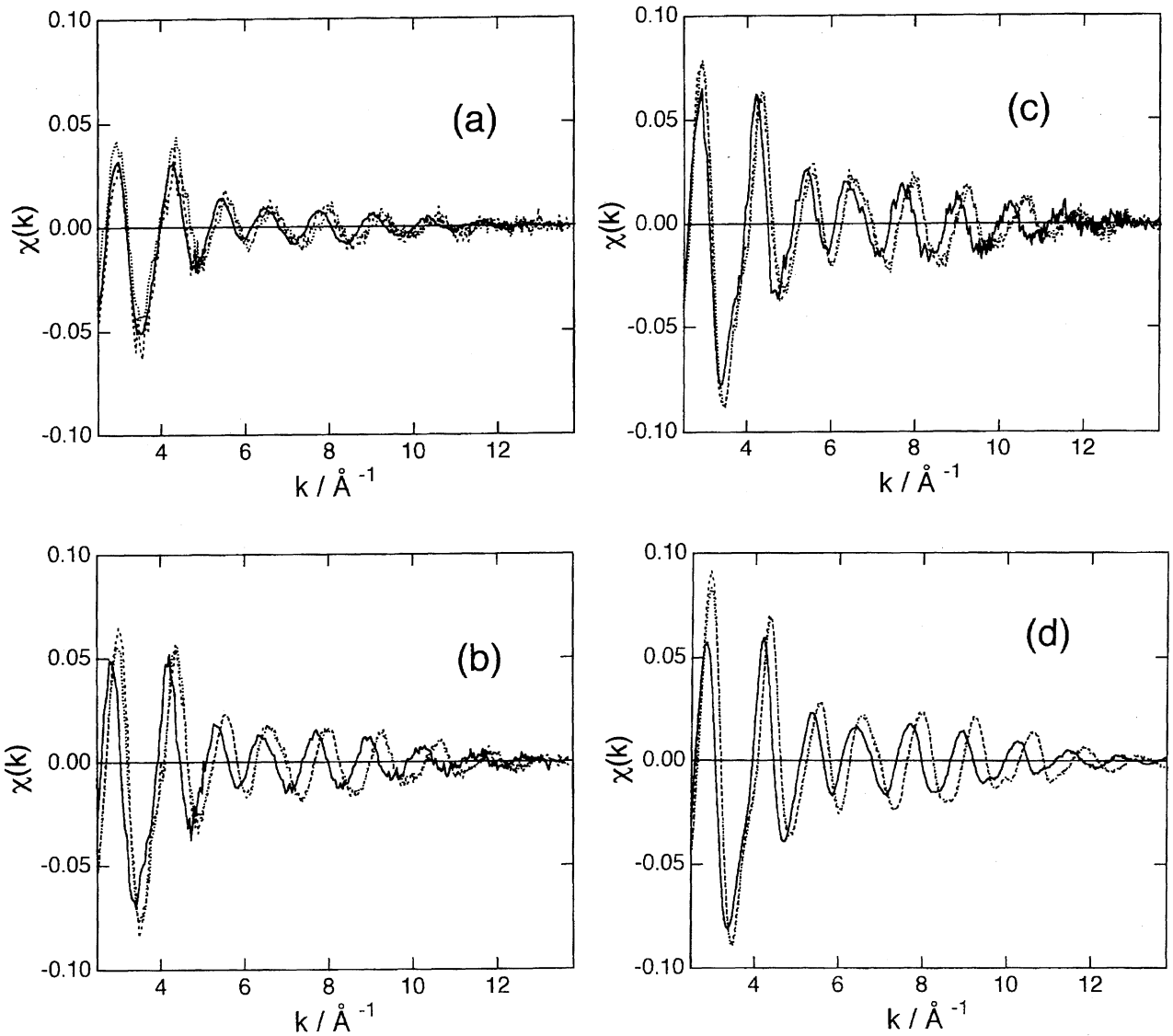

Fig. 1. Pd K-edge EXAFS oscillations ($\chi(k)$) for Pd/SiO_2 with the dispersion (H_{ad}/Pd) of 0.74 (a), 0.56 (b), 0.29 (c), and 0.12 (d); dotted line: Pd/SiO_2(VAC), solid line: $Pd/SiO_2(H_2)$; broken line: Pd/SiO_2(EVAC).

of dispersion (Figs. 3 and 4). The peak diminished by evacuation at room temperature, as shown in Figs. 3, 4, 5, and 6 for Pd/SiO_2(EVAC). On the other hand, the white line peak intensity increased by the evacuation at room temperature. For the samples with low dispersions ($H_{ad}/Pd = 0.12$ and 0.29), the intensity of the white line reverted to that for the corresponding Pd/SiO_2(VAC) samples. On the other hand, the white line peaks for the higher dispersion samples were smaller than those for the corresponding Pd/SiO_2(VAC) samples—due to the influence of chemisorbed hydrogen. Similar changes in XANES spectra were found for two Pd/Al_2O_3 samples with three different treatments. Namely, exposure of Pd/Al_2O_3($H_{ad}/Pd = 0.20$) to H_2 gas created a sharp peak at 3181 eV which decreased by the evacuation at room temperature. On the other hand the Pd/Al_2O_3 with $H_{ad}/Pd = 0.81$ (higher dispersion) showed a broad peak after the introduction of H_2 which was present even after the evacuation at room temperature.

To clarify these changes in XANES spectra, we took difference spectra. Figure 7 shows the difference spectra obtained by subtracting the spectra measured before hydrogen introduction (Pd/SiO_2(VAC)) from those for Pd/SiO_2(EVAC). The difference spectra between Pd/Al_2O_3(VAC) and Pd/Al_2O_3(EVAC) were also included in the figure. The new peak at about 3181 eV (about 8 eV above the inflection point of the edge) appeared in the difference spectra. The peak energy was independent of particle size and kind of support. Because the room temperature evacuation removes the absorbed hydrogen in the Pd bulk, the changes in these difference spectra are considered as the ones induced by the adsorbed hydrogen. The peak is denoted as ads-peak. The ads-peaks well correspond to the peaks in the Pt L-edge difference spectra between before and after H_2 adsorption on Pt particles.[16,17] The photon energy of the ads-peaks relative to the edge energy in Pd difference spectra is almost the same as that of the peaks observed in Pt L_3-edge difference spectra for the supported Pt samples.[16,17] Therefore, the ads-peaks in the Pd particles may have the same

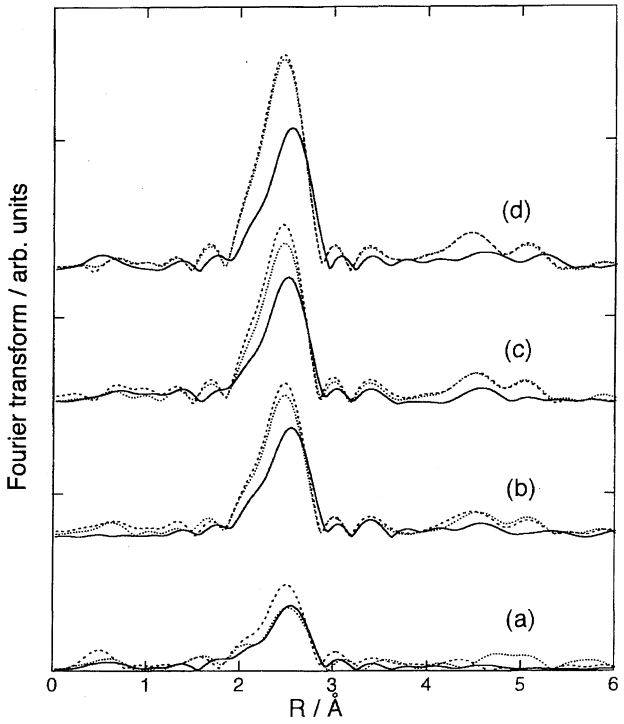

Fig. 2. Fourier transforms of k^3-weighted EXAFS for Pd/SiO_2 with the dispersion of 0.74 (a), 0.56 (b), 0.29 (c), and 0.12 (d); dotted line: Pd/SiO_2(VAC), solid line: $Pd/SiO_2(H_2)$; broken line: Pd/SiO_2(EVAC).

Table 3. Best-Fit Results for the EXAFS Data of Pd/SiO_2(VAC), $Pd/SiO_2(H_2)$, and Pd/SiO_2(EVAC)

H/Pd		N	R/nm	σ/nm	ΔE_0/eV	R_f/%
0.74	VAC	7±1	0.275±0.02	0.009±0.001	1±4	2.3
	H_2	6±1	0.281±0.02	0.009±0.001	1±3	0.9
	EVAC	5±1	0.277±0.02	0.007±0.001	0±4	2.3
0.56	VAC	9±1	0.275±0.02	0.007±0.001	0±3	1.1
	H_2	9±1	0.283±0.02	0.008±0.001	0±2	0.8
	EVAC	10±1	0.276±0.02	0.007±0.001	0±3	1.1
0.29	VAC	11±1	0.275±0.01	0.007±0.001	0±2	0.2
	H_2	11±1	0.283±0.01	0.008±0.001	3±2	0.3
	EVAC	11±1	0.276±0.01	0.007±0.001	1±3	0.8
0.12	VAC	12±2	0.275±0.02	0.007±0.001	−1±4	1.4
	H_2	12±2	0.284±0.02	0.008±0.001	0±3	1.0
	EVAC	12±2	0.275±0.02	0.007±0.001	−2±4	1.5

VAC: Pd/SiO_2 in vacuo (without exposure to H_2). H_2: Pd/SiO_2 under 13.3 kPa of H_2. EVAC: Pd/SiO_2 exposed to 13.3 kPa of H_2 and subsequently evacuated at room temperature for 1 h.

origin as the peaks found in hydrogen-adsorbed Pt particle samples. In the case of Pt particles, the peak intensity was proportional to the H/Pt value.[16,17] We plotted the intensity of the ads-peak against H_{ad}/Pd in Fig. 8.

Figure 9 shows the difference spectra obtained by subtracting the spectra of Pd/SiO_2(EVAC) from those of $Pd/SiO_2(H_2)$, together with corresponding spectra for Pd/Al_2O_3. The difference spectra are considered to indicate the change in the XANES spectra caused by hydrogen absorbed in the Pd bulk. The peak in the difference spectra appears at about 3181 eV (about 8 eV above the inflection point of the edge). This peak is denoted as abs-peak. The position of the abs-peaks referred to the edge position does not depend on the particle sizes and the kinds of support. The abs-peak appears at almost the same position as that of the ads-peaks. But, the abs-peaks are sharper than the ads-peaks. The abs-peak shows a relatively high intensity for the lower dispersion samples ($H_{ad}/Pd = 0.12$ and 0.29 for SiO_2 and $H_{ad}/Pd = 0.2$ for Al_2O_3) and the abs-peak for the higher dispersion becomes weaker and broader than that for lower dispersion.

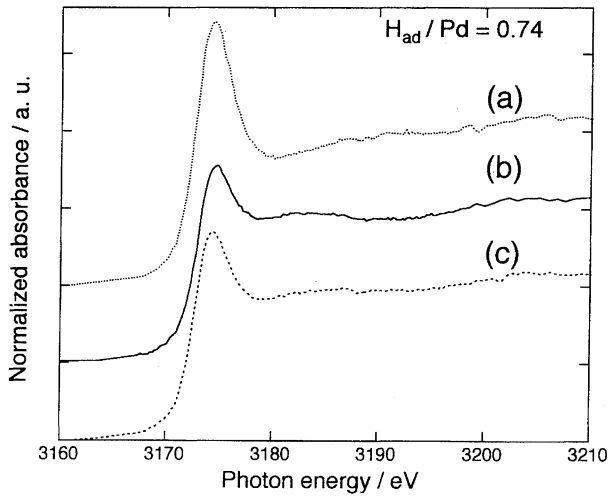

Fig. 3. Normalized Pd L_3-edge spectra for Pd/SiO_2 ($H_{ad}/Pd = 0.74$); (a) Pd/SiO_2(VAC), (b) $Pd/SiO_2(H_2)$, (c) Pd/SiO_2(EVAC).

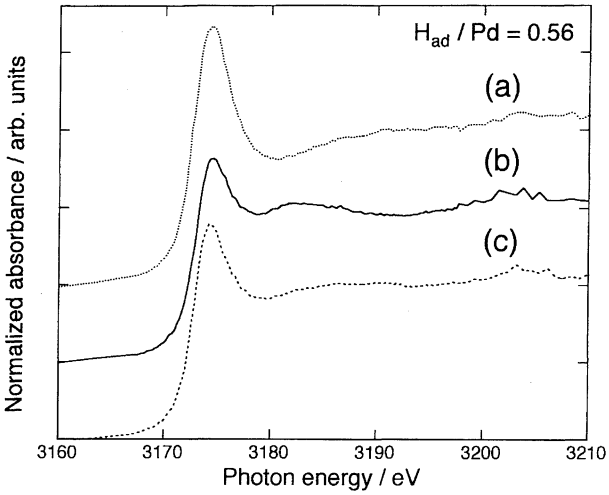

Fig. 4. Normalized Pd L_3-edge XANES spectra for Pd/SiO_2 ($H_{ad}/Pd = 0.56$); (a) Pd/SiO_2(VAC), (b) $Pd/SiO_2(H_2)$, (c) Pd/SiO_2(EVAC).

Discussion

Pd is known as a metal which absorbs many hydrogen atoms in the bulk to form hydride PdH_x. A disordered solution called α-phase is formed under low H_2 pressure at room

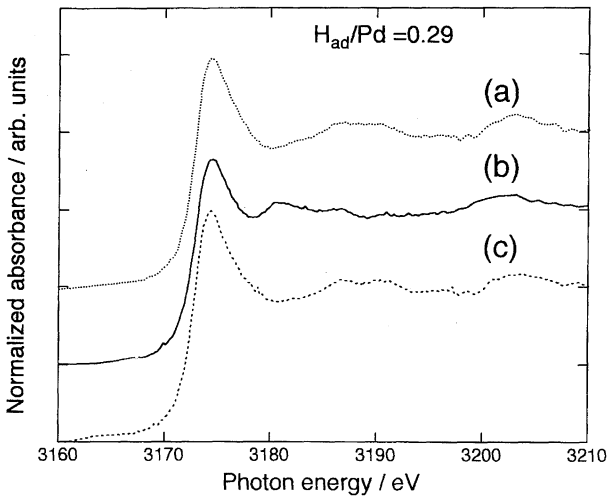

Fig. 5. Normalized Pd L_3-edge XANES spectra for Pd/SiO_2 ($H_{ad}/Pd = 0.29$); (a) Pd/SiO_2(VAC), (b) $Pd/SiO_2(H_2)$, (c) Pd/SiO_2(EVAC).

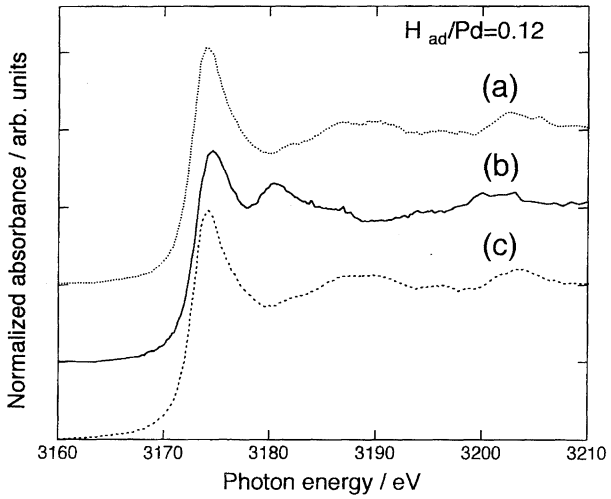

Fig. 6. Normalized Pd L_3-edge spectra for Pd/SiO_2 ($H_{ad}/Pd = 0.12$); (a) Pd/SiO_2(VAC), (b) $Pd/SiO_2(H_2)$, (c) Pd/SiO_2(EVAC).

temperature.[39] The Pd–Pd distance increases little in the α-phase. At higher H_2 pressures, α-phase is transformed to β-phase hydride and Pd–Pd distance is expanded to 0.2855 nm. The ratio of absorbed hydrogen to Pd at saturation is nearly 0.6 at room temperature. In the case of dispersed Pd particles where the fraction of surface Pd atoms is large, the amount of absorbed hydrogen atom per Pd atom (H_{ab}/Pd) is found to decrease.[30,31,35] Boudart and Hwang measured hydrogen absorption isotherms for Pd/SiO_2 with different particle sizes[35] and concluded that the H_{ab}/Pd decreased as the dispersion of Pd particles increased. They claimed H_{ab}/Pd would converge to zero at dispersion = 100%. Bonivardi et al. found that hydrogen solubility was suppressed with the larger dispersion of Pd particles.[30] But they reported that the H_{ab}/Pd became constant ($H_{ab}/Pd = 0.3$) at a dispersion larger than 0.6.

A characteristic peak appeared at about 8 eV above the edge in the Pd L_3-edge XANES spectra of a hydrogen-absorbing Pd thick film.[28] We found the peak at the same photon

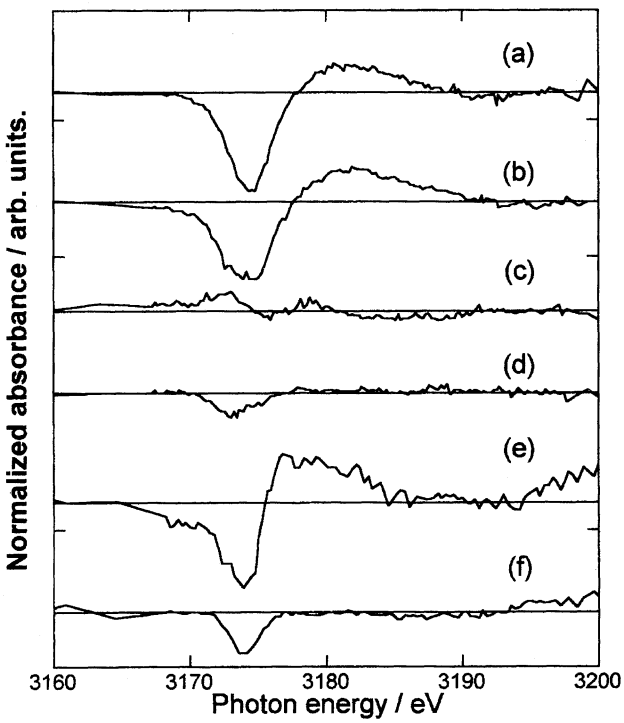

Fig. 7. Pd L_3-edge difference spectra for Pd/SiO_2 obtained by subtracting the spectra for Pd/SiO_2(VAC) from those for Pd/SiO_2(EVAC); (a) $H_{ad}/Pd = 0.74$, (b) $H_{ad}/Pd = 0.56$, (c) $H_{ad}/Pd = 0.29$, (d) $H_{ad}/Pd = 0.12$ and corresponding spectra for Pd/Al_2O_3 with (e) $H_{ad}/Pd = 0.81$, (f) $H_{ad}/Pd = 0.20$.

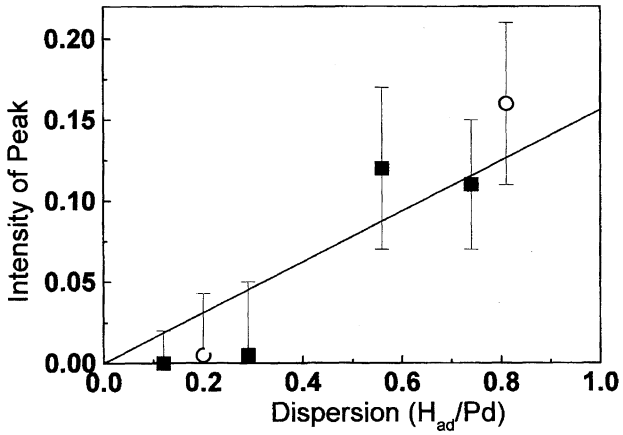

Fig. 8. Plots of the intensity of the ads-peak induced by adsorbed hydrogen against the dispersion (H_{ad}/Pd).

energy in the L_3-edge XANES spectrum for the Pd particles on SiO_2 with $H_{ad}/Pd = 0.12$ when they absorbed hydrogen. The peak position did not depend on the particle size or kind of support, indicating that the abs-peak is originating from the transition to a localized state such as Pd–H antibonding similar to the XANES peak in the chemisorbed hydrogen on Pt particles.[14–17] The peak height was a little smaller than that for the Pd films. The intensity of the abs-peak in the difference spectra between the spectra for $Pd/SiO_2(H_2)$ and Pd/SiO_2(EVAC) decreased with the decrease of particle size and the abs-peak almost disappeared in the case of Pd/SiO_2 with $H_{ad}/Pd = 0.74$. Furthermore, the intensities of the abs-

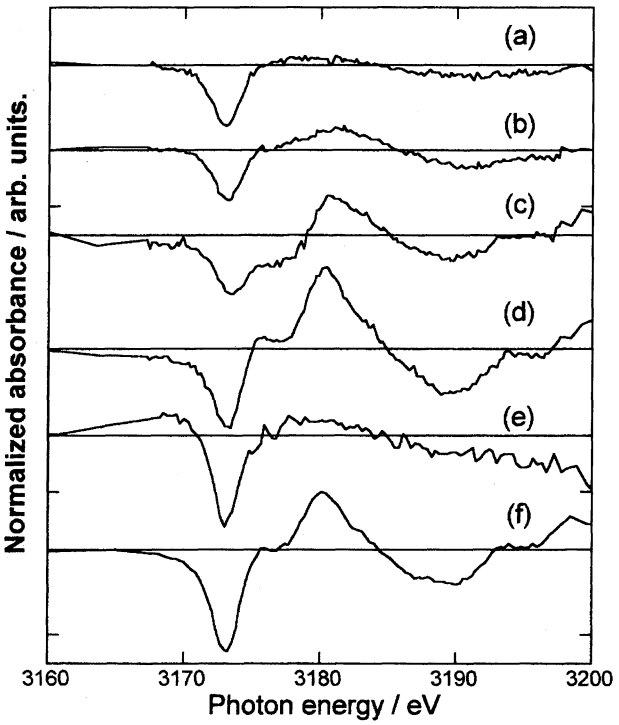

Fig. 9. Pd L_3-edge difference spectra for Pd/SiO_2 obtained by subtracting the spectra for Pd/SiO_2(EVAC) from those for $Pd/SiO_2(H_2)$; (a) $H_{ad}/Pd = 0.74$, (b) $H_{ad}/Pd = 0.56$, (c) $H_{ad}/Pd = 0.29$, (d) $H_{ad}/Pd = 0.12$ and corresponding spectra for Pd/Al_2O_3 with (e) $H_{ad}/Pd = 0.81$, (f) $H_{ad}/Pd = 0.20$.

peaks between $H_{ad}/Pd = 0.29$ and 0.12 were quite different. To explain the change of spectra, we assume that only bulk Pd atoms a few layers deeper than the surface give the abs-peak in the difference spectra. Hydrogen atoms located in intermediate layers between surface and bulk, called subsurface hydrogen atoms, do not modify the XANES spectra. We calculated the number of the bulk Pd atoms in the particle using a model shown in Fig. 10 where the Pd atoms at the location three layers deeper than the surface are regarded as the bulk Pd atoms, i.e., one-subsurface-layer model. The number of the bulk Pd atoms (Pd_b), the number of total Pd atoms (Pd_t), the number of surface Pd atoms (Pd_s), and the

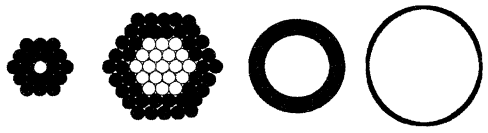

No. of shells*	N=2	N=4	N=8	N=24
$\frac{N_s}{N_t}$	0.74	0.56	0.29	0.12
$\frac{N_b}{N_t}$	0.03	0.16	0.46	0.77

* except the central atoms

Fig. 10. Models for Pd particles describing three regions (surface, subsurface and bulk), and the fractions of surface Pd atoms (Pd_s/Pd_t) and bulk Pd atoms (Pd_b/Pd_t).

number of subsurface Pd atoms (Pd_{ss}) are related to each other.

$$Pd_t = Pd_b + Pd_s + Pd_{ss},$$
$$Pd_s/Pd_t = H_{ad}/Pd, \quad (5)$$

Figure 11 shows correlation between the intensity of abs-peaks and the fraction of the bulk Pd atoms (Pd_b/Pd_t) calculated based on the model of Fig. 10. The peak intensity for H-absorbed Pd film which can be regarded as $Pd_b/Pd_t = 1$ is also plotted using the literature data.[28] We also plotted the peak intensity for H-absorbed Pd/Al_2O_3 samples. We can find a linear relation between the abs-peak intensity and Pd_b/Pd_t in Fig. 11 irrespective of the kind of support. We also calculated other models with different numbers of near surface layers. Figure 11 includes the plots for no subsurface and two-subsurface-layer model where Pd atoms deeper than two layers and four layers were regarded as bulk atoms, respectively. In the no subsurface-layer model, we did not obtain a linear relation between the intensity of abs-peak and Pd_b/Pd_t as shown in Fig. 11. Although the two-subsurface-layer model could give a linear correlation between them, the line did not go through the bulk value ($Pd_b/Pd_t = 1$). These results indicate that surface (top layer) and subsurface (second layer) Pd atoms interact with hydrogen atoms in a different manner from the bulk part of Pd atoms.

The presence of "subsurface" hydrogen with different nature from the bulk hydrogen has been demonstrated by kinetics, TDS, LEED, He scattering, ARUPS and theoretical work and the subsurface hydrogen is considered to be in a distinct intermediate state for the transformation of chemisorbed hydrogen(surface) to absorbed one(bulk).[40—55] The TPD spectra revealed that subsurface hydrogen on Pd(110) surface

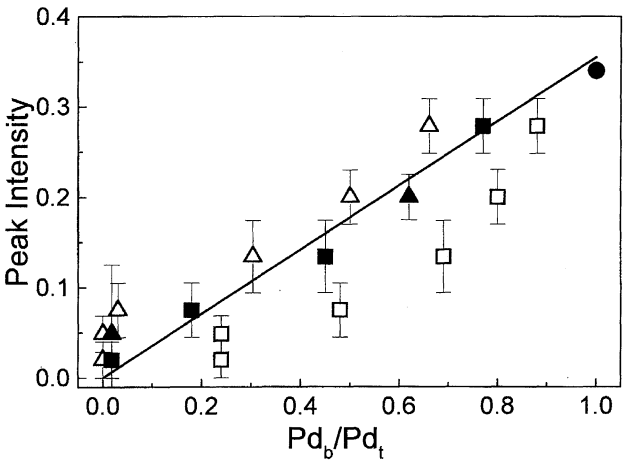

Fig. 11. Plots (filled square) of the intensity of abs-peak of Pd/SiO_2 against Pd_b/Pd_t calculated from the one-subsurface-layer model of Fig. 10. The Pd_b/Pd_t values calculated from no subsurface-layer (open square) and two-subsurface-layer (open triangle) models are also plotted. Filled circle indicates peak intensity estimated from the spectra in Ref. 28. Filled triangles indicated the correponding intensity of abs-peak for Pd/Al_2O_3 against Pd_b/Pd_t based on one-subsurface-layer model.

have a different desorption energy from the energies for chemisorbed and absorbed hydrogen.[48] The Pd–H bond in the subsurface region may be different in bond length and electronic structure from that in the bulk region. In fact the present EXAFS data for the Pd particles with smaller sizes which had surface and subsurface hydrogen atoms showed the smaller Pd–Pd bond expansion. The multiple scattering calculation for absorbed H–Pd particle suggested that the abs-peak appears only when the Pd–Pd distance was expanded and hydrogen had a positive charge.[56] Thus it is concluded that the abs-peak originates from the hydrides dissolved in the bulk part of Pd particles (from the third layer), that the interaction of subsurface and surface hydrogen with Pd is different from that of the bulk hydride, and that subsurface hydrogen atoms do not change the Pd L_3-edge XANES spectra.

On the other hand, the difference spectra between Pd/SiO_2(VAC) and Pd/SiO_2(EVAC) show the change originating from the hydrogen atoms adsorbed on the Pd surface. It was found that the ads-peak by the surface hydrogen atoms appeared at 8 eV above the edge (Fig. 7). The energy of the ads-peaks was independent of the particle size and kind of support. The peak position of the ads-peaks was similar to that of the abs-peaks but the shape of the ads-peaks was relatively broadened. A similar peak has been observed in the Pt $L_{2,3}$-edge XANES spectra for hydrogen-adsorbed Pt particles.[16,17] The ads-peaks at 8 eV above the edges in the white lines at Pt and Pd L_3-edges can be explained by the multiple scattering scheme. Ohtani et al. calculated the XANES of hydrogen-adsorbed Pt particles using the multiple scattering theory and found that the peak appears when the charge transfer occurs from Pt 6s to H 1s.[15] They also calculated Pd particles with adsorbed hydrogen[56] and found that the adsorption of hydrogen changes the XANES spectra but the spectra are not so sensitive to the electron structures of the Pd and adsorbed H atoms, in contrast to the Pt case. It was found that there is a positive correlation between the ads-peak intensity and the Pd dispersion, as shown in Fig. 8.

Conclusions

1. A new peak (abs-peak) in the XANES spectra for hydrogen absorbed Pd particles was observed. The peak intensity increased with the size of Pd particles, which indicates that absorbed hydrogen atoms in the Pd bulk can be quantified by the abs-peak in XANES.

2. The Pd–H bonding in the subsurface region did not contribute to the abs-peak.

3. A new peak (ads-peak) at 8 eV higher than the edge in difference spectra was also observed for hydrogen-adsorbed Pd/SiO_2 and Pd/Al_2O_3. The ads-peak corresponds to that found in small Pt particles.

4. The ads-peak intensity had a positive correlation with the Pd dispersion (H_{ad}/Pd) and the amount of adsorbed hydrogen at the Pd surface.

5. A model of Pd particles composed of surface, subsurface and bulk for the adsorption and absorption of hydrogen was presented by the analysis of the Pd L_3-edge XANES spectra for Pd/SiO_2(VAC), $Pd/SiO_2(H_2)$, and Pd/SiO_2(EVAC).

This work has been supported by CREST (Core Research for Evolutional Science and Technology) of Japan Science and Technology Corporation (JST). The XANES measurements have been done with the approval of the Photon Factory advisory committee (PAC) (Proposal No. 95G380).

References

1) N. Kosugi, in "X-Ray Absorption Fine Structure for Catalysis and Surface," ed by Y. Iwasawa, World Scientific, Singapore (1996), Vol. 2, p. 60.
2) T. Fujikawa, in "X-Ray Absorption Fine Structure for Catalysis and Surface," ed by Y. Iwasawa, World Scientific, Singapore (1996), Vol. 2, p. 76.
3) M. Brown, R. E. Peierls, and E. A. Stern, *Phys. Rev. B*, **15**, 738 (1977).
4) F. W. Lytle, P. S. P. Wei, R. B. Greegor, G. H. Via, and J. H. Sinfelt, *J. Chem. Phys.*, **70**, 4849 (1979).
5) J. A. Horsley, *J. Chem. Phys.*, **76**, 1451 (1982).
6) A. N. Mansour, J. W. Cook, and D. E. Sayers, *J. Phys. Chem.*, **88**, 2330 (1984).
7) H. Yoshitake and Y. Iwasawa, *J. Phys. Chem.*, **95**, 7368 (1991).
8) N. Ichikuni and Y. Iwasawa, *Catal. Lett.*, **20**, 87 (1993).
9) F. W. Lytle, R. B. Greegor, E. C. Marques, D. R. Sandstrom, G. H. Via, and J. H. Sinfelt, *J. Catal.*, **95**, 546 (1985).
10) M. G. Samant and M. Boudart, *J. Phys. Chem.*, **95**, 4070 (1991).
11) M. Vaarkamp, J. T. Miller, F. S. Modica, and D. C. Koningsberger, *Jpn. J. Appl. Phys.*, **32**, 454 (1993).
12) P. G. Allen, S. D. Conradson, M. S. Wilson, S. Gottesfeld, I. D. Raistrick, J. Valerio, and M. Lovato, *Electrochim. Acta*, **39**, 2415 (1994).
13) S. N. Reifsnyder, M. M. Otten, D. E. Sayers, and H. H. Lamb, *J. Phys. Chem. B*, **101**, 4972 (1997).
14) N. Watari and S. Ohnishi, *J. Chem. Phys.*, **106**, 7531 (1997).
15) K. Ohtani, T. Fujikawa, T. Kubota, K. Asakura, and Y. Iwasawa, *Jpn. J. Appl. Phys.*, **36**, 6504 (1997).
16) K. Asakura, T. Kubota, N. Ichikuni, and Y. Iwasawa, in "Stud. Surf. Sci. Catal.," ed by J. W. Hightower, W. N. Delgass, E. Iglesia, and A. T. Bell, Elsevier Science, Amsterdam (1996), Vol. 101, p. 911.
17) T. Kubota, K. Asakura, N. Ichikuni, and Y. Iwasawa, *Chem. Phys. Lett.*, **256**, 445 (1996).
18) T. Kubota, K. Asakura, and Y. Iwasawa, *Catal. Lett.*, **46**, 141 (1997).
19) W. Palczewska, *Adv. Catal.*, **24**, 245 (1975).
20) R. K. Nandi, R. Pitchai, S. S. Wong, J. B. Cohen, R. L. Burwell, Jr., and J. B. Butt, *J. Catal.*, **70**, 298 (1981).
21) R. K. Nandi, P. Georgopoulos, J. B. Cohen, J. B. Butt, J. R. L. Burwell, and D. H. Bilderback, *J. Catal.*, **77**, 421 (1982).
22) G. Carturan, G. Facchin, G. Cocco, S. Enzo, and G. Navazio, *J. Catal.*, **76**, 405 (1982).
23) E. Rorris, J. B. Butt, R. L. Burwell, and J. B. Cohen, "Proc. 8th Inter. Congre. Catal.," Berlin (1984), Abstr., IV-321.
24) R. Dus, *Surf. Sci.*, **50**, 241 (1975).
25) J. M. Moses, A. H. Weiss, K. Matusek, and L. Guczi, *J. Catal.*, **76**, 405 (1984).

26) W. Palczewska, in "Hydrogen Effects in Catlaysis," ed by Z. Paal and P. G. Menon, Marcel Dekker, New York (1988), Vol. 31, p. 373.
27) J. M. Orozco and G. Webb, *Appl. Catal.*, **6**, 67 (1983).
28) I. Davoli, A. Marcelli, G. Fortunato, A. D'amico, C. Coluzza, and A. Bianconi, *Solid State Commun.*, **71**, 383 (1989).
29) A. V. Soldatov, S. D. Longa, and A. Bianconi, *Solid State Commun.*, **85**, 863 (1993).
30) A. L. Bonivardi and M. A. Baltans, *J. Catal.*, **138**, 500 (1992).
31) J. E. Benson, H. S. Hwang, and M. Boudart, *J. Catal.*, **30**, 146 (1973).
32) T. Ohta, P. M. Stefan, M. Nomura, and H. Sekiyama, *Nucl. Instrum. Method*, **A246**, 373 (1986).
33) M. Funabashi, T. Ohta, T. Yokoyama, Y. Kitajima, and H. Kuroda, *Rev. Sci. Instrum.*, **60**, 2505 (1989).
34) K. Asakura, in "X-Ray Absorption Fine Structure for Catalysts and Surfaces," ed by Y. Iwasawa, World Scientific, Singapore (1996), Vol. 2, p. 33.
35) M. Boudart and H. S. Hwang, *J. Catal.*, **39**, 44 (1975).
36) K. Inukai, K. Asakura, and Y. Iwasawa, *J. Catal.*, **143**, 22 (1993).
37) R. B. Greegor and F. W. Lytle, *J. Catal.*, **63**, 476 (1980).
38) M. G. Mason, *Phys. Rev. B*, **27**, 748 (1983).
39) Z. Paal and P. G. Menon, "Hydrogen Effects in Catalysis," Marcel Dekker, New York (1988).
40) A. W. Aldag and L. D. Schmidt, *J. Catal.*, **22**, 260 (1971).
41) J. F. Lynch and T. B. Flanagan, *J. Phys. Chem.*, **77**, 2628 (1973).
42) W. Auer and H. J. Grabke, *Ber. Bunsenges. Phys. Chem.*, **78**, 58 (1974).
43) J. A. Konvalinka and J. J. Scholten, *J. Catal.*, **48**, 374 (1977).
44) S. G. Louie, *Phys. Rev. Lett.*, **42**, 476 (1979).
45) W. Eberhardt, F. Greuter, and E. W. Plummer, *Phys. Rev. Lett.*, **46**, 1085 (1981).
46) M. G. Cattania, V. Penka, R. J. Behm, K. Christmann, and G. Ertl, *Surf. Sci.*, **126**, 382 (1983).
47) W. Eberhardt, S. G. Louie, and E. W. Plummer, *Phys. Rev. B*, **28**, 465 (1983).
48) R. J. Behm, V. Penka, M.-G. Cattania, K. Christamnn, and G. Ertl, *J. Chem. Phys.*, **78**, 7486 (1983).
49) K. H. Rieder, M. Baumberger, and W. Stocker, *Phys. Rev. Lett.*, **51**, 1799 (1983).
50) C. T. Chan and S. G. Louie, *Phys. Rev. B*, **30**, 4153 (1984).
51) M. Baumberger, W. Stock, and K. H. Rieder, *Appl. Phys.*, **A41**, 151 (1986).
52) T. E. Felter, S. M. Foiles, M. S. Daw, and R. H. Stulen, *Surf. Sci.*, **171**, L379 (1986).
53) M. S. Daw and S. M. Foiles, *Phys. Rev. B*, **35**, 2128 (1987).
54) R. A. Olsen, P. H. T. Philipsen, and E. J. Baerends, *J. Chem. Phys.*, **106**, 9286 (1997).
55) R. A. Olsen, G. J. Kroes, O. M. Løvvik, and E. J. Baerends, *J. Chem. Phys.*, **107**, 10652 (1997).
56) K. Ohtani, T. Fujikawa, T. Kubota, K. Asakura, and Y. Iwasawa, *Jpn. J. Appl. Phys.*, **37**, 4134 (1998).